# Original Article

# Formulation and Characterization of Lacosamide-loaded Polymeric Microneedles

Kadir Aykaç[1,2] and Ebru Başaran[1*]

[1]*Department of Pharmaceutical Technology, Faculty of Pharmacy, Anadolu University, Eskişehir, Turkey;* [2]*Department of Pharmaceutical Technology, Faculty of Pharmacy, Erzincan Binali Yıldırım University, Erzincan, Turkey*

## Abstract

**Background and objectives:** Epilepsy is a neural disorder that occurs because of a disruption in neural conductions in various parts of the brain and is mainly characterized by seizures, pensive gaze, involuntary mimics, contractions, meaningless speeches, repetitive movements, and loss of consciousness. The serious side effects of conventional drug delivery systems due to high applied doses, low transition rates to the brain, and limitations of drug application during seizures result in the urgent need for novel drug delivery systems for the enhanced treatment of epilepsy.

**Methods:** In this study, Lacosamide was selected because of its high therapeutic dose, which is due to its low transition to the target site. Microneedle patches were formulated by micromolding of polymers of carboxymethyl cellulose (CMC) and Eudragit S 100 (ES100) for a unique route for applications to reduce the applied dose to minimize the severe side effects. This strategy enhanced brain transition via the nasal route and overcame the blood-brain barrier (BBB) to minimize the applied dose. Characterization studies were performed in detail.

**Results:** The results revealed that the releases of Lacosamide extended to 96 h with ES100 microneedle patches. In contrast, CMC microneedles released almost all the active ingredients within 1 h due to the hydrophilic nature of the polymer. Stability studies indicated that the formulations were stable at 25 ± 2°C (60 ± 5% Relative Humidity; RH), 40 ± 2°C (75 ± 5% RH) and 5 ± 3°C for 6 months.

**Conclusions:** By considering the film like structures, polymeric microneedle patches have the potential for Lacosamide delivery through the unconventional nasal route for the improved treatment of epilepsy.

## Introduction

Epilepsy is a neurological disorder that occurs due to the imbalanced production of stimulant and inhibitory signals in neurons in the brain. The stimulant signal production is more than the inhibitory signals by dysfunctional neurons and can cause seizures in patients.[1] Epilepsy affects >45 million people of different ages worldwide.[2,3] Epilepsy is attributed to brain defects, specific genetic factors, infections, metabolic disorders, immune dysfunctions, accidental injury, and idiopathic reasons.[4,5] Lacosamide is an active R enantiomer of 2-acetamido-N-benzyl-3-methoxypropionamide (of which the S enantiomer is inactive) and has been approved for the treatment of focal (partial-onset) seizures as a
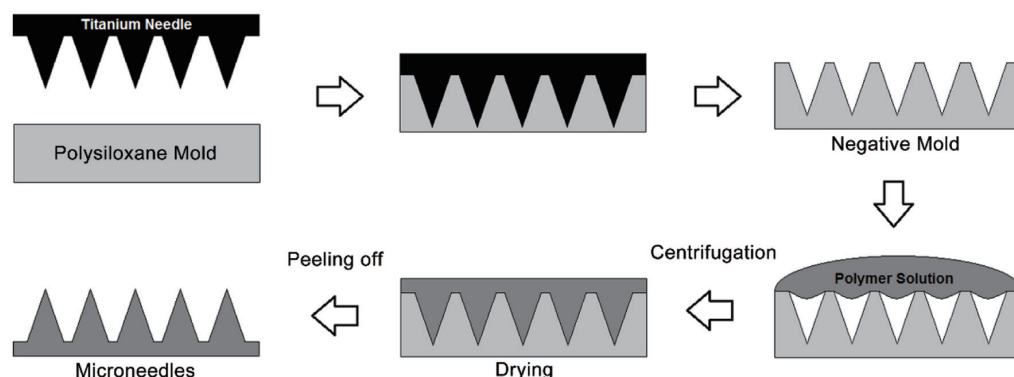
**Fig. 1. Microneedle production with micromolding method.**

monotherapy and adjunctive therapy in the European Union and the US.[6,7] Lacosamide can reduce the frequency of seizures in epilepsy patients. Treatment starts with 50 mg Lacosamide twice a day and can be increased ≤200–600 mg daily according to the frequency of seizures and tolerance of the patients.[8] Lacosamide is a functionalized amino acid, which is known as harcoseride, with anticonvulsant and antinociceptive properties.[9] Lacosamide is an analog of D-serine that has amphiphilic properties, which allow the molecule to be water-soluble enough to be formulated into a parenteral product and lipophilic enough to cross the blood-brain barrier (BBB).[8] However, although Lacosamide has high oral bioavailability, it has a low transition rate into the brain via the oral route.[10,11] Nasal drug delivery is an alternative route for the enhanced bioavailability of most drugs.[12] Although the nasal route is thought to provide a local treatment in the first place, it gives the potential to deliver active agents for systemic treatment and to circumvent the BBB through the olfactory pathway.[13] The nasal route can rapidly deliver the drugs, which overcomes the first-pass effect and results in comparable bioavailability profiles with infusion. Therefore, the nasal route is an alternative application route for systemic drug delivery with higher patient compliance, compared with parenteral applications.[14,15]

Microneedles are commonly designed for the transdermal route to enhance skin penetration and avoid the pain that usually occurs with parenteral administration, and can be formulated for other routes of application, such as ocular and nasal routes.[16] Microneedles can be classified as solid, coated, hollow, hydrogel-based, and dissolving microneedles.[17–20] Microneedles can be produced by many methods, such as lithography,[21] droplet air blowing,[22] and micromolding methods.[23] The method for microneedle production mainly depends on the type of material or polymer used.[17,24–26] In this study, thin microneedle patches were formulated by micromolding,[23] for an unconventional route of microneedle application to reduce the applied dose of Lacosamide, minimize the severe side effects, and enhance brain transition.

## Methods

### Materials

Lacosamide was provided by Santa Farma (Istanbul, Turkey). Carboxymethyl cellulose sodium salt (CMC) and hydroxylpropyl gamma-cyclodextrin (HPGCD) were purchased from Sigma-Aldrich (Steinheim, Germany). Eudragit S 100 (ES100) was purchased from Röhm Pharma (Darmstadt, Germany). Polyethylene

glycol (PEG) 400, acetonitrile, o-phosphoric acid, methanol, and ethanol were purchased from Merck (Darmstadt, Germany). All other chemicals were of analytical grade.

### Production of microneedle patches

Microneedle patches were prepared by micromolding.[23] The molds were constructed using the polysiloxane Zetaplus C Silicone Kit (Rovigo, Italy) (polysiloxane:activator, [10:1]; w/w). Dermapen® needles (Biberach, Deutschland) were used as a master template for the microneedles (Fig. 1). After formation of the molds briefly, 75 mg of ES100 was dissolved in 1 mL of methanol, which was mixed with 5 μL PEG 400 as a plasticizer. For CMC-based formulations, 60 mg of CMC and 20 mg of HPGCD were dissolved in 1 mL of distilled water. Different concentrations of Lacosamide were added to the solutions. The solution samples (500 μL each) were poured into the molds and centrifuged three times (4,000 rpm, 10 m) to maintain complete settlement of the solution in the tiny gaps. The molds were evaporated at 40 ± 1°C for 24 h. The microneedle patches were gently peeled off the polysiloxane molds and stored in sealed containers.[21,27] Placebo formulations were prepared without the addition of Lacosamide.

### Morphological analyses

The morphological properties of the microneedle patches were investigated by scanning electron microscopy (SEM) analyses that used Zeiss Ultra Plus FE-SEM (Oberkochen, Germany).

### Thermal analyses

Structural and crystallinity changes in Lacosamide and other ingredients and the polymeric structure of the microneedle patches were evaluated using differential scanning calorimetry (DSC) (DSC-60, Shimadzu Scientific Instruments, Colombia, US). Analyses were performed under a nitrogen atmosphere (50 mL/min) at 30–300°C with an increase rate of 10°C/min. An empty aluminum pan was used as a reference.

### Fourier-transform infrared analyses

Fourier-transform infrared spectroscopy was used to further analyze the structure of the microneedle patches (FTIR) IR Affinity-

1S Shimadzu, Tokyo, Japan) using a high-sensitivity Deuterated Lanthanum α Alanine doped TriGlycine Sulphate (DLaTGS) detector with a Germanium-coated KBr Beam splitter from 7,800 to 350 cm⁻¹.

### Nuclear magnetic resonance analyses

The interactions between the active agent and the polymers were analyzed by nuclear magnetic resonance ($^1$H-NMR) with Fourier 300 NMR (Bruker Bioscience, MA, US).

### Texture analyses

Insertion studies were determined with TA.XT-plus Texture Analyzer (Stable Micro Systems, Surrey, UK) using Parafilm as the membrane simulant material.[28,29] The microneedle patches were bonded to the tip of the Texture Analyzer's mucoadhesion probe with double-sided tape. Parafilm was folded into eight layers (1 mm thick) and fixed on a flat block of aluminum base. The compression mode was chosen in the Texture Analyzer's program then pretest speed, test speed, and post-test speed were adjusted to 1.0, 0.05, and 10.0 mm/sec, respectively. The microneedle attached to the probe was lowered onto the folded Parafilm and 5, 10, 15, 25, 35, and 42 N forces were applied on different samples for 15 s. Parafilm samples were examined under a stereomicroscope Leica M205 (Leica, Wetzlar, Germany) to determine the insertion depths of the needles.

### Determination of Lacosamide

The Lacosamide content in the microneedle patches was determined by a modified high-performance liquid chromatography (HPLC) method[30] in a Shimadzu 20 A (Tokyo, Japan) with an Agilent C18 column (column diameter: 4.6 mm, column length: 25.0 cm, particle diameter: 5 μm, and particle size: 100 Å; Santa Clara, US). Acetonitrile:distilled water: o-phosphoric acid (40:59:1 v/v and pH 2.0 ± 0.0) was used as the mobile phase with a flow rate of 1.0 mL/min. Then, 20 μL volumes of the samples were injected via an autosampler (SIL-20A, Shimadzu, Tokyo, Japan) and a photodiode array detector (SPD-M20A, Shimadzu, Tokyo, Japan) was used at 210 nm. The column temperature was set to 40 ± 1°C (CTO-10AS-VP, Shimadzu, Tokyo, Japan).[30] Validation studies were performed.[31]

### Drug loading capacity

The microneedles (10 mg) were dissolved in 2 mL methanol or water for ES100 and CMC-based microneedles, respectively. The solutions were filtered through presaturated polyamide membrane filters and supernatants were analyzed by HPLC after proper dilutions (n=3). Drug loading capacity was calculated according to Equation 1.[32]

$$\text{Drug loading (\%)} = [(\text{Lacosamide weight}) / (\text{microneedle weight})] \times 100 \qquad (1)$$

### In vitro drug release and its kinetics

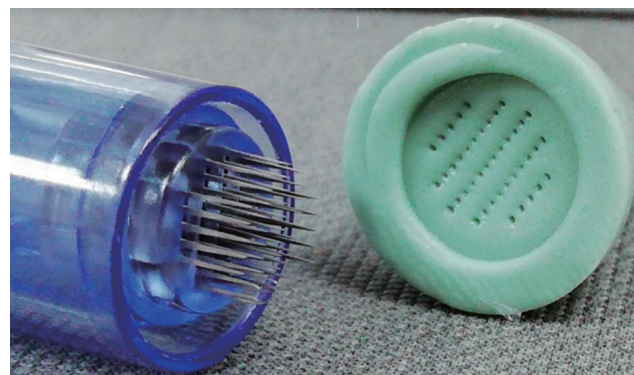The microneedle patches were dissolved in a phosphate buffer



**Fig. 2. Master template (left) and microneedle mold (right) for micromolding method.**

solution (PBS, pH 6.4) for *in vitro* drug release studies.[33] The microneedle patches were attached to round-shaped magnets and fixed in the 50 mL buffer solution (under sink conditions, 37±1°C and 150 rpm stirring) with the help of an external second magnet to maintain the release of Lacosamide from the surface of the patches.[34] The samples (1 mL each) were taken at certain time points and 1 mL fresh buffer solution was added to maintain sink conditions. The collected samples were analyzed by HPLC after proper dilution when required. The *in vitro* release kinetic modeling of the microneedle patches was analyzed using the DD-Solver software program.[35]

### Stability of microneedles

The microneedle patches were maintained under three different conditions: 25 ± 2°C (60 ± 5% RH); 40 ± 2°C (75 ± 5% RH); and 5 ± 3°C for 6 months to determine the stability of the formulations.

## Results

### Production of microneedles

In this study, microneedle molds were produced using the Zeta-plus C Silicone Kit. Titanium Dermapen® needles were used as a master template for the formation of the gaps for the microneedles. Molds were 9 mm in diameter with a 1.5 mm needle height and 42 micro hollows for the needles (Fig. 2). In preliminary studies, Eudragit derivatives (e.g., R 100, L 100, RL 100, RS 100, RL PO, RS PO, RL PM, and RS PM), chitosan (high molecular weight), sodium alginate, and polyvinylpyrrolidone (PVP) were used for the formulation of microneedles. According to the initial evaluations, the CMC and ES100-based formulations were selected for further studies (Table 1).

### Morphological analyses

The morphology of the microneedles with length, shape, and diameter information was revealed with SEM analyses (Fig. 3).[36] Microneedle heights could be adjusted at the mold formation stages, which depended on the preferred route of application. The microneedles formulated with ES100 were 1,270–1,500 μm in length and 250–300 μm in diameter and the CMC-based microneedles

**Table 1. Compositions and Lacosamide amounts in the microneedles (Mean ± SE, n = 3)**

| Code | CMC (%) | HPGCD (%) | ES100 (%) | PEG 400 (%) | Lacosamide, Theoretical (%) | Lacosamide, Practical (%) |
|------|---------|-----------|-----------|-------------|------------------------------|----------------------------|
| EL0 | – | – | 7.5 | 0.5 | – | – |
| EL1 | – | – | 7.5 | 0.5 | 0.5 | 0.61 ± 0.00 |
| EL2 | – | – | 7.5 | 0.5 | 1.0 | 1.07 ± 0.03 |
| EL3 | – | – | 7.5 | 0.5 | 1.5 | 1.53 ± 0.00 |
| CL0 | 6.0 | 2.0 | – | – | – | – |
| CL1 | 6.0 | 2.0 | – | – | 0.5 | 0.56 ± 0.01 |
| CL2 | 6.0 | 2.0 | – | – | 1.0 | 1.10 ± 0.01 |
| CL3 | 6.0 | 2.0 | – | – | 1.5 | 1.56 ± 0.01 |

CMC, pure carboxymethyl cellulose; HPGCD, hydroxylpropyl gamma cyclodextrin; ES100, Eudragit S 100; PEG 400, polyethylene glycol 400.

were 1,300–1,500 μm in length and 100–250 μm in diameter, respectively.

### Thermal analyses

In DSC analyses, Lacosamide displayed an endothermic melting peak at 149°C, which was due to the crystalline structure (marked with arrows), and ES100 and CMC exhibited no endothermic melting peaks in the thermograms, which showed the amorphous structures of the polymers (Fig. 4). DSC thermograms of placebo and Lacosamide-loaded microneedle patches were evaluated, and the formulations displayed similar behavior with pure polymers, which highlighted the amorphous structures of the microneedles.

### Fourier-transform infrared analyses

Lacosamide has characteristic absorption peaks at 1,633 cm$^{-1}$ and 3,286 cm$^{-1}$ that correspond to the stretching vibrations of C=O and N-H, respectively.[37] The characteristic absorption peaks of Lacosamide were revealed in the spectrum of both physical mixtures and Lacosamide was compatible without any interaction with both of the formulation components (marked with arrows) (Fig. 5). The FTIR spectrum of ES100 indicated that the peak at 2,926 cm$^{-1}$ was due to the presence of O-H groups (carboxylic acid) at approximately 1,450 cm$^{-1}$, which was due to -CH$_3$ bending, and at 1,724 cm$^{-1}$, which was due to the presence of C=O (ester)[38] and -C-O-C stretching vibrations at 1,150 cm$^{-1}$.[39] CMC had a strong characteristic absorption band at 1,022 cm$^{-1}$ that was due to the carboxymethyl ether group (CHOCH$_2$$^{-}$) and displayed a broad absorption band at 3,352 cm$^{-1}$, that was due to the stretching frequency of -OH groups[40] and peaks that were observed at 1,595 cm$^{-1}$ and 1,605 cm$^{-1}$ were due to the C=O region of CMC.[41]

### Nuclear magnetic resonance analyses

$^1$H-NMR analyses were performed to determine the molecular interactions (Fig. 6).[42] Two different solvents [deuterated dimethyl sulfoxide (DMSO) for ES100 and deuterium oxide (DOx)] for CMC-based microneedles were used for analyses that considered the different solubility properties of the polymers. The characteristic peaks of ES100 were found at 12–13 ppm. Lacosamide signals were detected in the spectra of the microneedles at approximately 2.0, 4.0–4.5, and 7.5–8.0 ppm (marked with arrows) (Fig. 6).

### Texture analyses

Insertion studies were performed with Texture Analyzer on Parafilm as the membrane simulant material with different application forces.[28,29] M205 (Leica, Wetzlar, Germany) was used to determine the insertion depths of the needles under different penetration forces (Fig. 7) and stereomicroscope images of the third layer of Parafilm with the highest application force of 42N were shown in Figure 8.

### Determination of Lacosamide

HPLC validation was carried out following the ICH guidelines within the range of 5–100 μg/mL.[31] In linearity studies, r$^2$ was 0.9999, the accuracy values were in the range of 100.1–101.4%, and relative standard deviation (RSD) was <2% for the precision studies. The selectivity of the method was analyzed compared with placebo microneedle formulations (e.g., EL0 and CL0) and with all the components of this study.

### Drug loading capacity

Lacosamide concentration in the microneedles was evaluated by validated HPLC analyses. The analyses results revealed that the Lacosamide concentrations were very close to the theoretical Lacosamide concentrations in the microneedles (Table 1).

### In vitro drug release and release kinetics

*In vitro* drug release studies were performed in PBS (pH 6.4) for 96 h to determine the release profiles of Lacosamide from the polymeric microneedles. Because CMC is water-soluble, the majority of the Lacosamide was released within 1 h from the CMC-based microneedles. Considering the low aqueous solubility of ES100-based microneedles, approximately only 20–25% of cumulative releases were achieved at 96 h (Fig. 9).[43,44]

### Stability of microneedles

During the stability studies, the formulations were monitored at 25 ± 2°C (60 ± 5% RH), 40 ± 2°C (75 ± 5% RH), and 5 ± 3°C
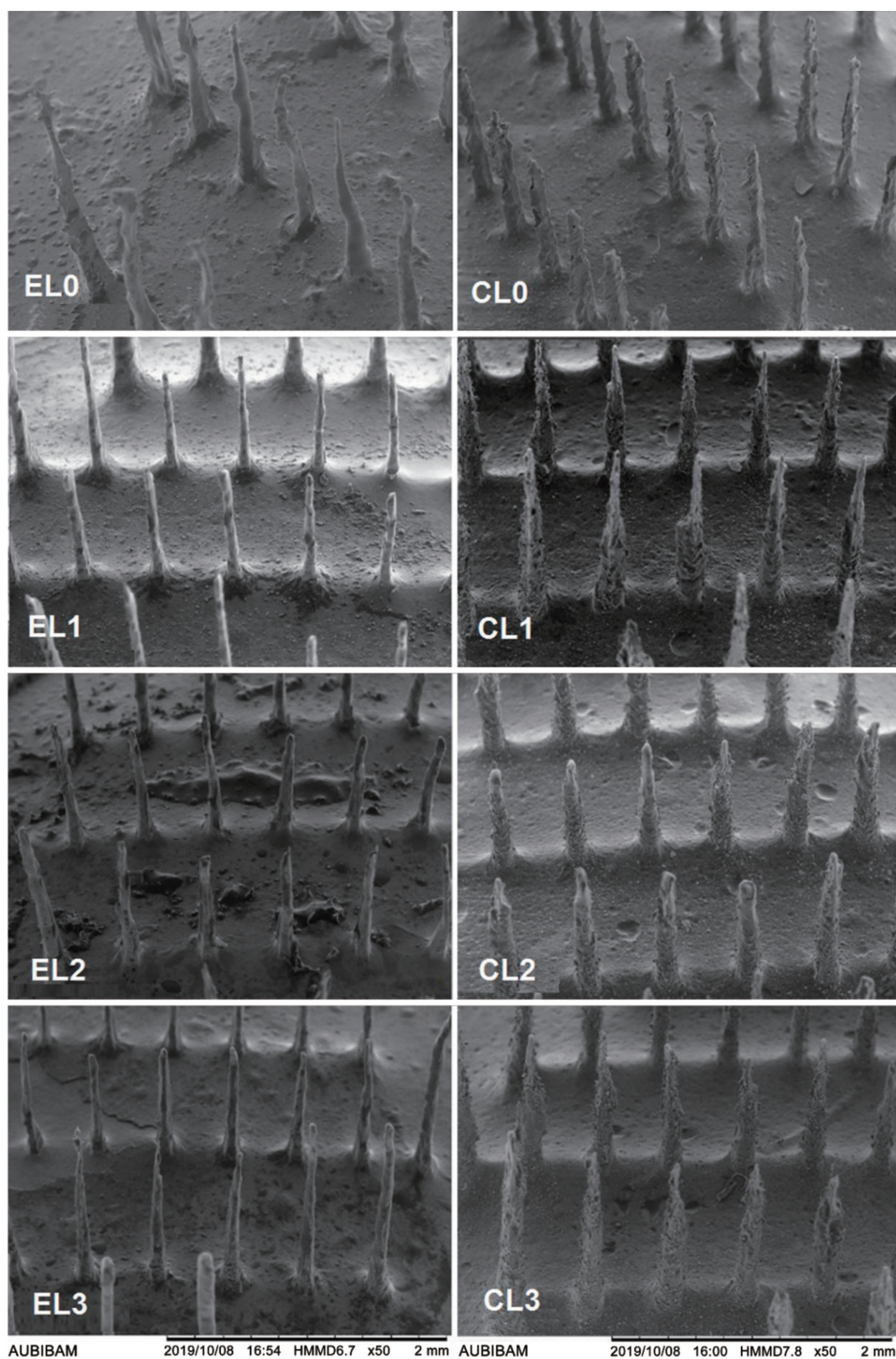
**Fig. 3. SEM images of microneedle patches [Left column Eudragit S 100 (ES100) based formulations (EL0, EL1, EL2, and EL3) and right column carboxymethyl cellulose (CMC) based formulations (CL0, CL1, CL2, and CL3)].**
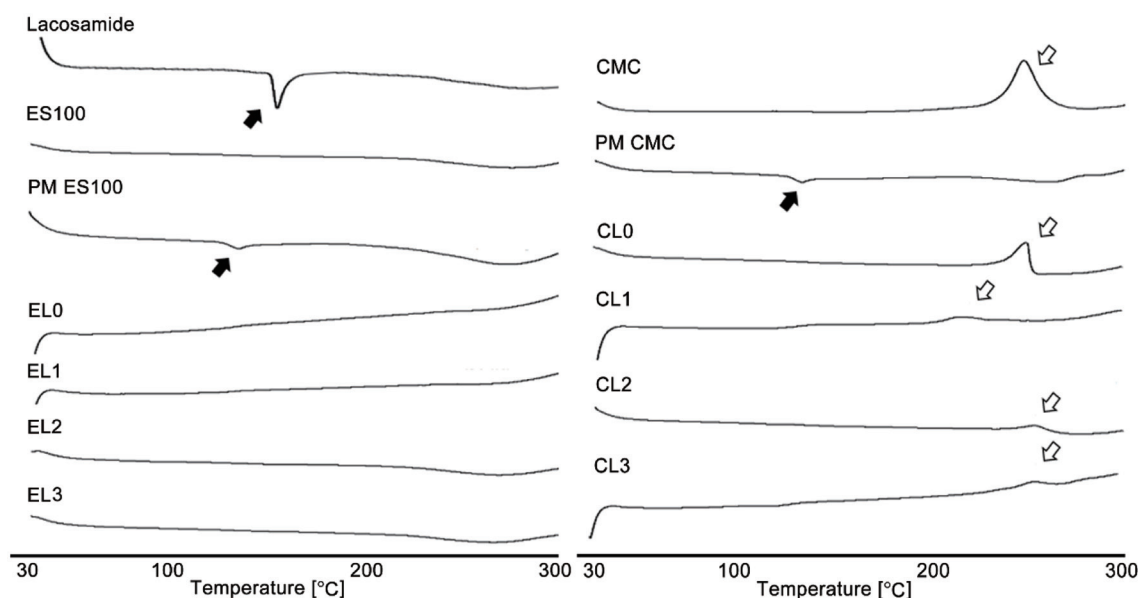
**Fig. 4. DSC thermograms of pure materials and microneedle formulations: ES100, pure Eudragit S 100; PM ES100, physical mixture of ES100 based formulations components; EL0, EL1, EL2, and EL3, ES100 based formulations; CMC, pure carboxymethyl cellulose; PM CMC, physical mixture of CMC-based formulations components; CL0, CL1, CL2, and CL3, CMC-based formulations.** Endothermic melting peaks of Lacosamide are marked with black arrows and decomposition peaks of CMC are marked with hollow arrows.

and the Lacosamide amount, FTIR, and ^{1}H-NMR analyses were performed at the end of 6 months.[45] To minimize the numbers analyzed, a bracketing approach was used for the stability studies, and therefore, only the EL1, EL3, CL1, and CL3 formulations were monitored. Minor changes in Lacosamide concentrations were observed and the changes remained under the limit of 5%, which showed the stability of all the formulations under all storage conditions (Fig. 10).[45]

FTIR analyses stated that there was no change in the specific signals of Lacosamide and all of the microneedles remained stable during storage under these storage conditions (Fig. 11). ^{1}H-NMR analyses results also revealed that different storage conditions did not influence the characteristic signals of the microneedles during storage for 6 months in agreement with the FTIR analyses results (Fig. 12).

## Discussion

The film layer for the polymers was one of the most important factors for the selection of the polymers for the microneedle formulations.[46] The strength and flexibility of the film layers were very important when peeling them off the molds and during the application of the microneedles. CMC is a water-soluble anionic cellulose derivative, which is commonly used in pharmaceutical formulations,[47] and ES100 is a pH-dependent soluble polymer (pH>7) commonly used in colon-targeted drug delivery systems.[48] To determine the influence of polymer solubility on the release of Lacosamide, water-soluble and water-insoluble microneedles were formulated with CMC and ES100, respectively. The composition of the formulations were different for the different properties of pure polymeric films. PEG 400 was added to ES100 formulations to enhance the flexibility of the microneedles, which was required to peel off the Eudragit based microneedle patches from the molds and HPGCD was added to the CMC formulations to maintain the higher strength rates, which were very important for the insertion

performance of the microneedles through the membranes.[49]

In characterization studies the SEM analyses results revealed that CMC microneedles had thinner and smoother surfaces than ES100 microneedles. In addition, Lacosamide concentrations did not influence the microneedle morphology at the studied concentrations. With the help of sharp ended needles, it could be easier to deliver the Lacosamide through the nasal mucosa effectively with both patches (Fig. 3).[50] In DSC analyses amorphous structures of the polymers were revealed while Lacosamide displayed a crystalline structure. Physical mixtures were evaluated to determine the solubility properties and interactions between the formulation components. The Lacosamide melting peak was revealed in the thermograms of the physical mixtures (marked with arrows), and Lacosamide and the components had no incompatibility problems (Fig. 4).[51] In addition, a decomposition peak was determined at approximately 260°C in thermogram of CMC and CMC-based microneedles, which was consistent with previous studies (marked with hollow arrows) (Fig. 4).[52,53] DSC thermograms of placebo and Lacosamide-loaded microneedle patches were evaluated, and the formulations displayed similar behavior with pure polymers, which highlighted the amorphous structures of the microneedles. Since the melting peak of Lacosamide disappeared in the thermograms of the formulations, Lacosamide was no longer in crystalline form within the polymeric structure for the ES100 and CMC microneedle formulations (Fig. 4).[51,54] FTIR spectroscopy was used to investigate the interactions between Lacosamide and the formulation components in the microneedle patches.[55] The characteristic signals of Lacosamide were detected in the spectra of the formulations, and the active agent was molecularly dispersed within the polymer, which was consistent with DSC analyses without any chemical transformation (marked with arrows) (Fig. 5). Lacosamide peaks became apparent based on the increased amount of the active agent (marked with arrows) in the CMC microneedles and no chemical transformations were revealed during formulation stages (Fig. 5). ^{1}H-NMR analyses were performed to determine the molecular interactions and Lacosamide
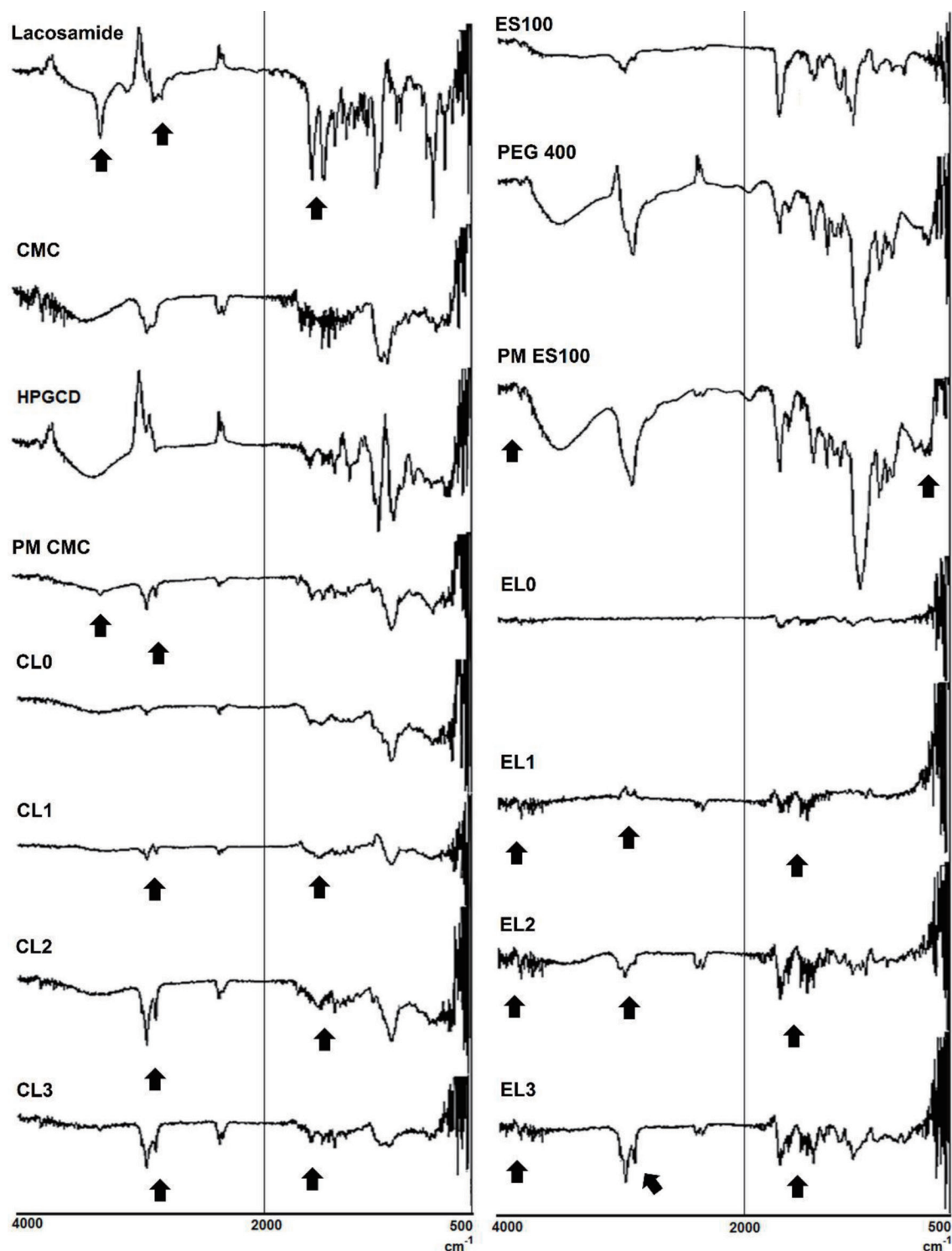
**Fig. 5. FTIR spectra of pure materials and microneedle formulations.** ES100, pure Eudragit S 100; PEG 400, polyethylene glycol 400; PM ES100, physical mixture of ES100 based formulations components; EL0, EL1, EL2, and EL3, ES100 based formulations; CMC, pure carboxymethyl cellulose; HPGCD, hydroxylpropyl gamma cyclodextrin; CMC, physical mixture of CMC-based formulations components; CL0, CL1, CL2, and CL3, CMC-based formulations.

signals were detected in the spectra of the microneedles at approximately 2.0, 4.0–4.5, and 7.5–8.0 ppm (marked with arrows), which indicated the presence of Lacosamide within the polymeric network

without any chemical interactions (Fig. 6). Texture analyses results revealed that only the CL0 formulation effectively passed through all the layers of Parafilm with the most robust structure. The rest of
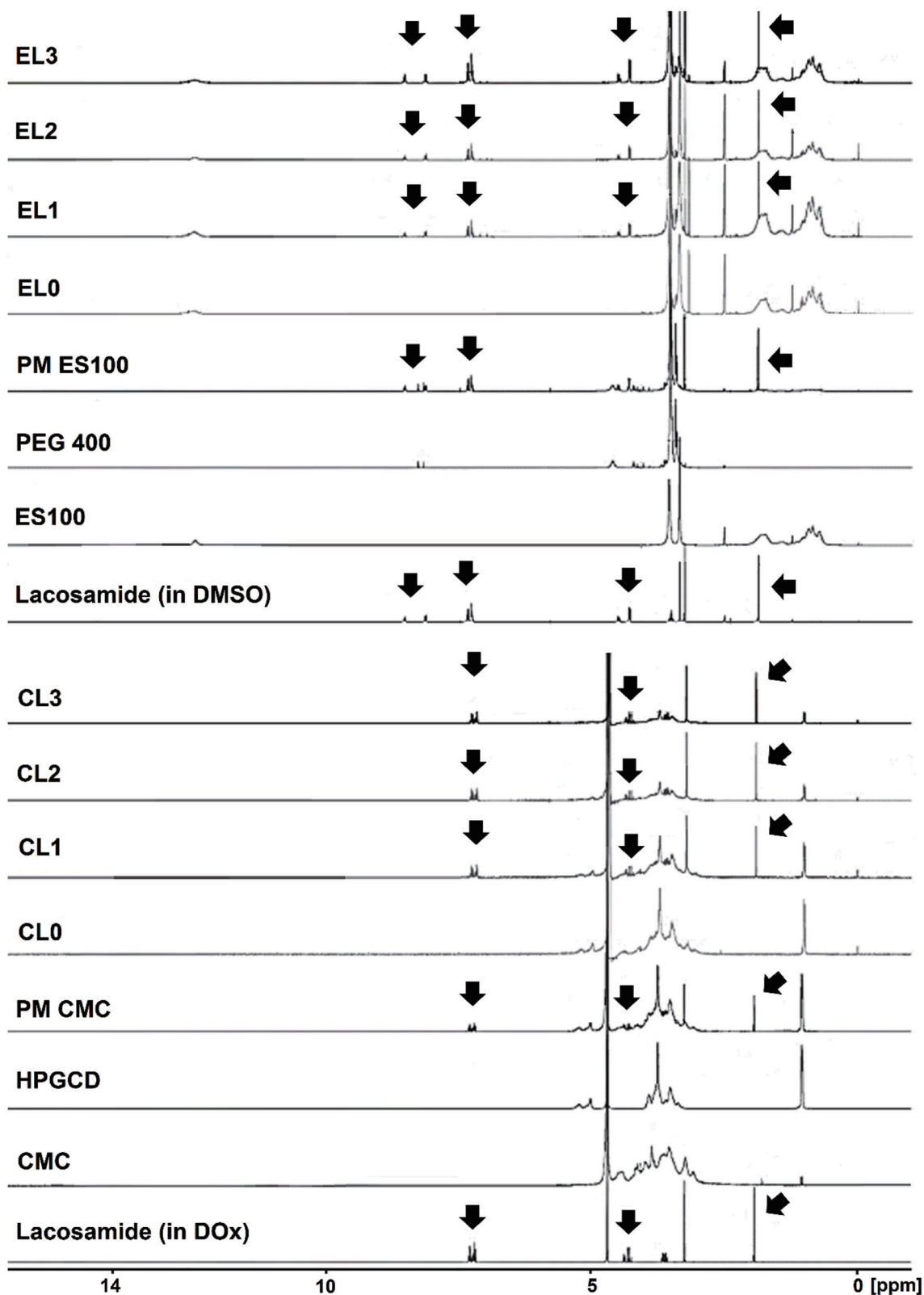
**Fig. 6. ¹H-NMR spectra of pure materials and microneedle formulations.** ES100, pure Eudragit S 100; PEG 400, polyethylene glycol 400; PM ES100, physical mixture of ES100 based formulations components; EL0, EL1, EL2, and EL3, ES100 based formulations; CMC, pure carboxymethyl cellulose; HPGCD, hydroxyl-propyl gamma cyclodextrin; CMC, physical mixture of CMC-based formulations components; CL0, CL1, CL2, and CL3, CMC-based formulations.
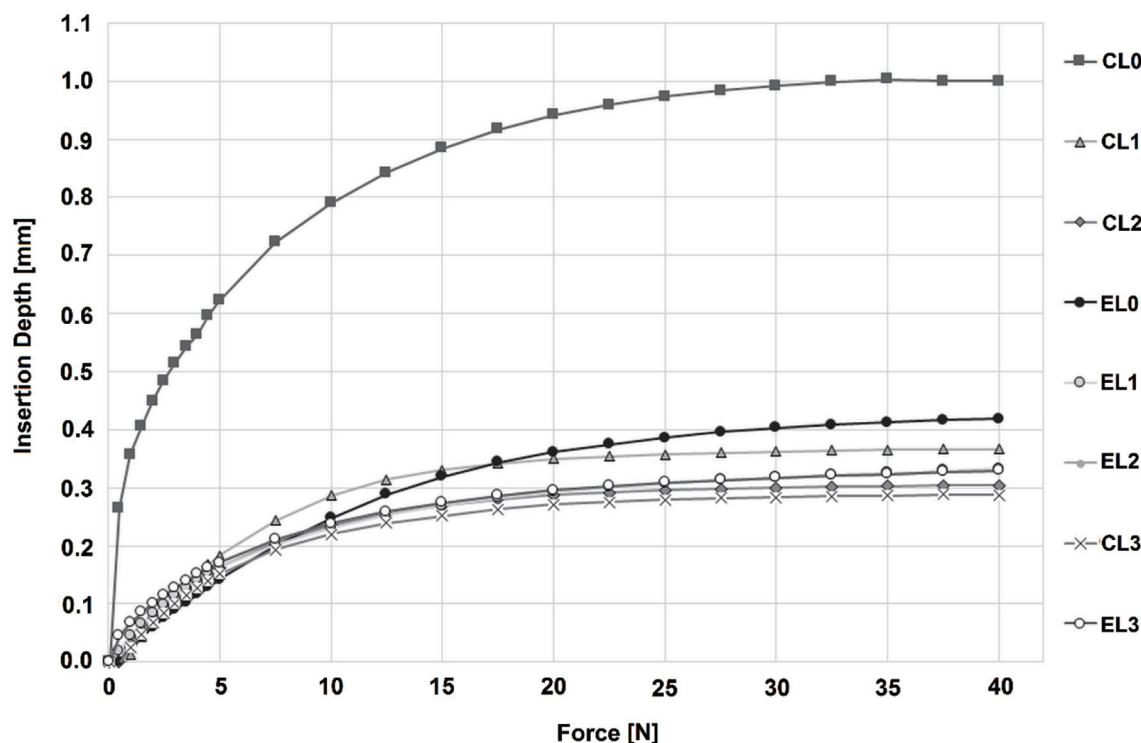
**Fig. 7. Insertion depths of the microneedles under different puncture forces (Mean ± SE; n = 3).** EL0, EL1, EL2, and EL3, Eudragit S 100 based formulations; CL0, CL1, CL2, and CL3, carboxymethyl cellulose-based formulations.

the samples reached the third layer of Parafilm; however, CL1 and EL0 reached the fourth layer (0.5 mm) with broken needles (Fig. 7). Stereomicroscope images revealed the successful penetration of the microneedles (Fig. 8). *In vitro* drug release studies were performed in PBS (pH 6.4) for 96 h and due to CMC is water-soluble, the majority of the Lacosamide was released within 1 h from the CMC-based microneedles. Considering the low aqueous solubility of ES100-based microneedles, approximately only 20–25% of cumulative releases were achieved at 96 h (Fig. 9).[43,44] The analyses results revealed that the type of the polymer had a major influence on the release rates of the incorporated drug; therefore, the polymeric mixtures could maintain the required sustained releases within the preferred time frames (Fig. 9).[56] *In vitro* release analysis results were evaluated by the DDSolver Program to determine the release characteristics of the microneedles. Best-fitted pharmacokinetic models were selected that considered the smaller Akaike Information Criterion (AIC), largest Model Selection Criterion (MSC), and highest Determination Coefficient (R2) values, which were stated as the most defined parameters for the evaluation of the release kinetics.[35] The analyses results revealed that EL1, EL2, and all the CMC-based formulations fitted to the Korsmeyer-Peppas kinetic model, which describes the release of a drug from a polymeric matrix.[57,58] The Lacosamide and EL3 formulations fitted the first-order kinetic model, which is dependent on the concentrations of the drug.[58,59]

During the stability studies, minor changes in Lacosamide concentrations were observed however the changes remained under the limit of 5% (Fig. 10).[45] FTIR and ^{1}H-NMR analyses are the most important analyses methods for the determination of minor structural changes in polymeric drug delivery systems.[60–62] In our study the specific signals of Lacosamide remained unchanged in all microneedle patches under all storage conditions in both FTIR and ^{1}H-NMR (Figs. 11, 12). Stability studies stated that the mi-

croneedle patches remained stable under all storage conditions during storage period of 6 months.

## Future directions

In this study, formulation, *in vitro* characterization studies, and stability studies on Lacosamide-loaded CMC and ES100 polymeric microneedle patches were performed. For better evaluations of the performances of the prepared formulations *in vivo* studies are required. The animal models for the determination of *in vivo* performance are challenging. The regular animals used for *in vivo* studies, such as mice and rats, are easy to handle; however, their nasal cavities are small. Therefore, large animals, such as sheep, might be valuable for unconventional application routes for microneedles. Depending on the selected animal model, needle heights should be adjusted at the molding stage.

## Conclusions

The present study described the formulation and characterization of Lacosamide-loaded CMC and ES100-based polymeric microneedle patches with micromolding. The *in vitro* characterization results revealed that the structural properties of the microneedles were unique and the microneedles were stable to store for 6 months at 25 ± 2°C (60 ± 5% RH), 40 ± 2°C (75 ± 5% RH), and 5 ± 3°C. The CMC-based microneedles released Lacosamide at the highest point within 1 h and the ES100 based microneedles released only approximately 20–25% cumulative levels at 96 h. Therefore, Lacosamide release could be optimized for immediate
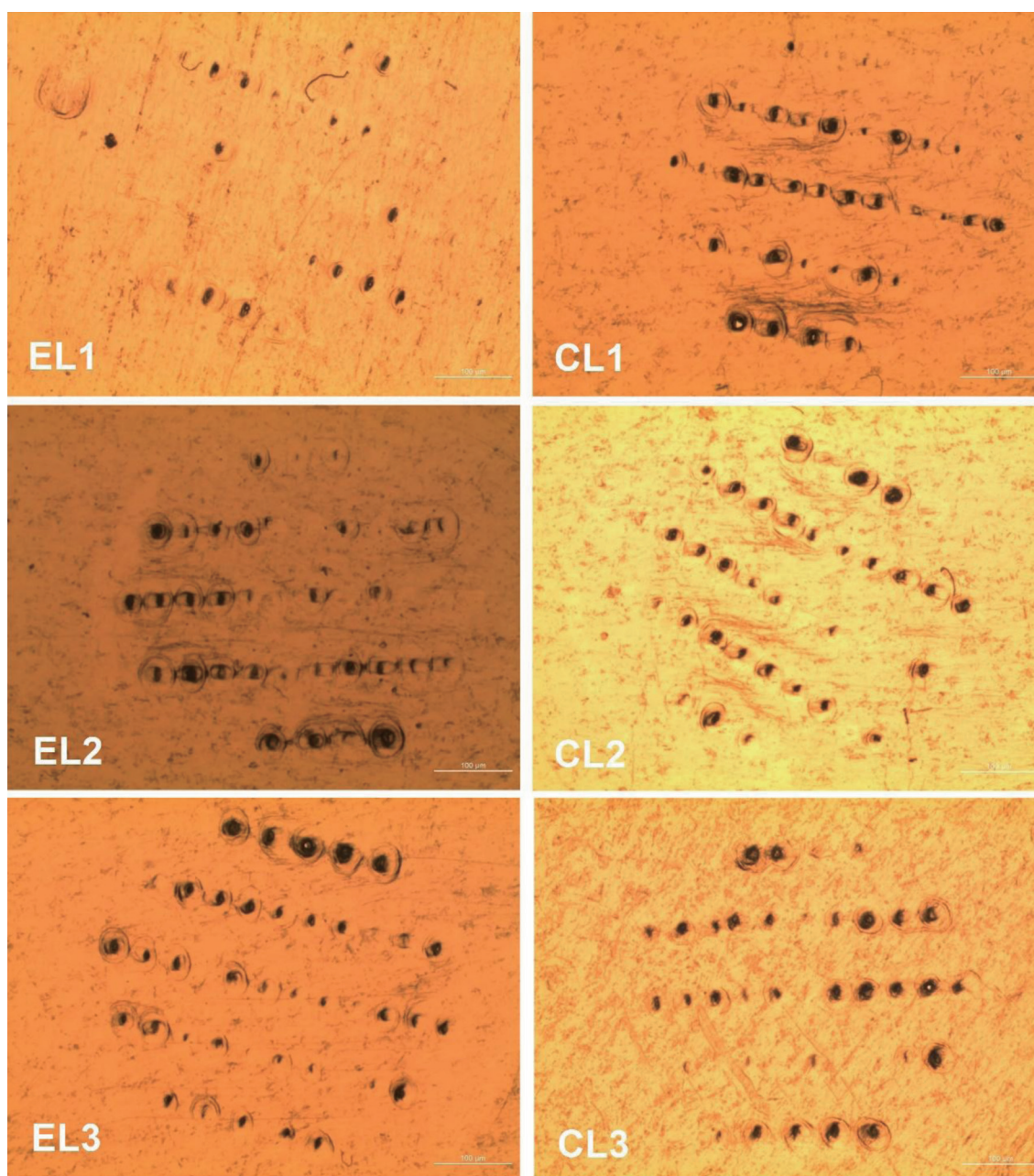
**Fig. 8. Stereo microscope images of the third layer of Parafilm under 42 N puncture force.** EL0, EL1, EL2, and EL3, Eudragit S 100 based formulations; CL0, CL1, CL2, and CL3, carboxymethyl cellulose-based formulations.

or sustained releases upon the required targeted therapies. Future research will determine *in vivo* studies on the formulations to deliver Lacosamide via the nasal route for an improved treatment for epilepsy to overcome the BBB in a less invasive way.

### Conflict of interest

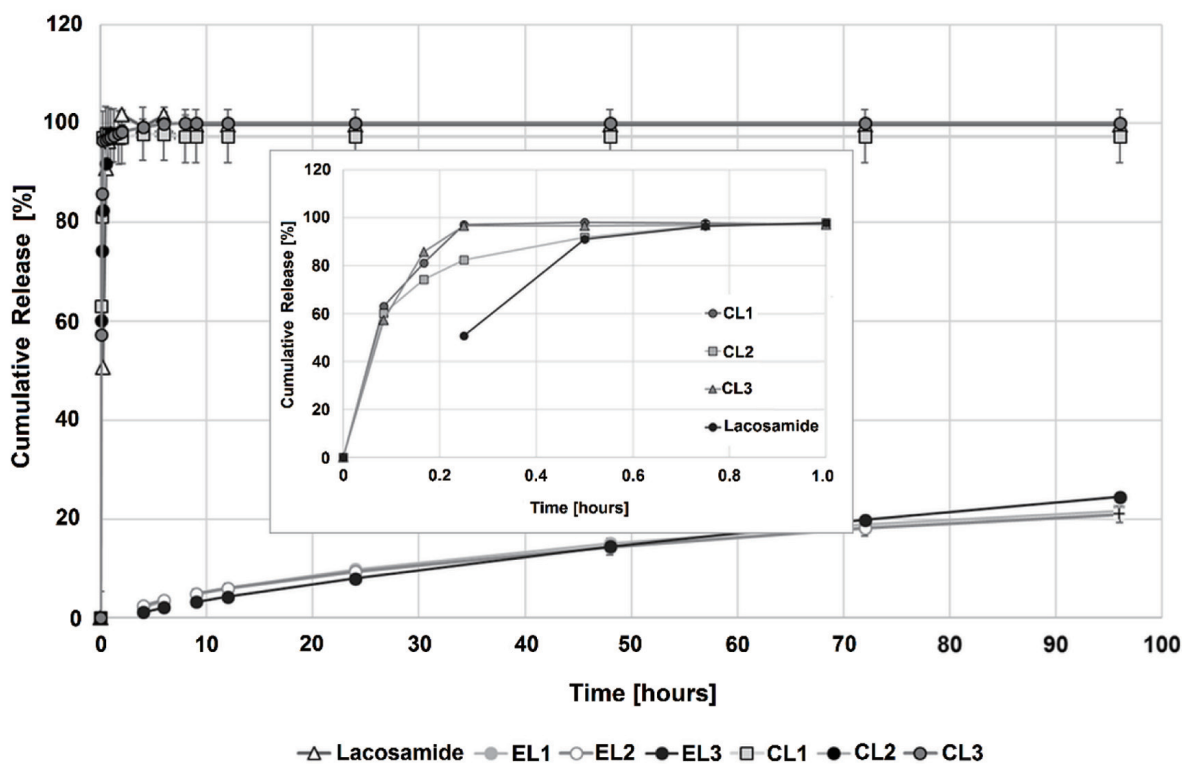Dr Ebru Başaran has been an editorial board member of the *Journal*

**Fig. 9. *In vitro* drug release of Lacosamide from microneedles (Mean ± SE; n = 3).** EL1, EL2, and EL3, Eudragit S 100 based formulations; CL1, CL2, and CL3, carboxymethyl cellulose-based formulations.



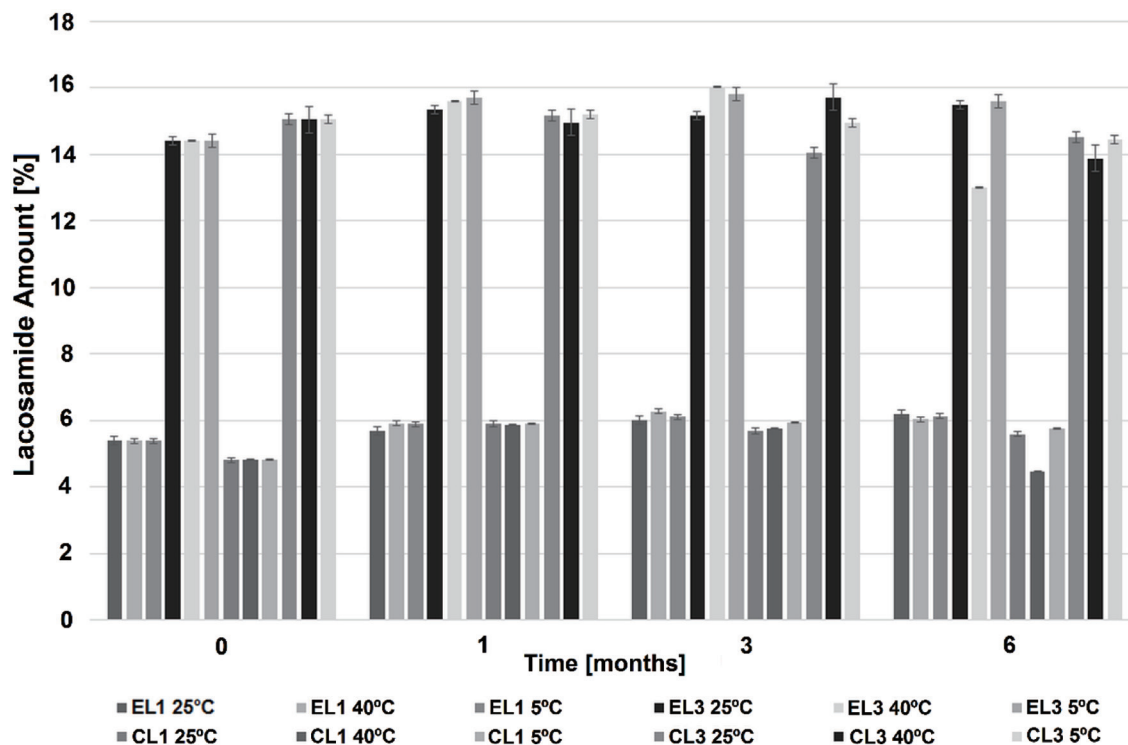**Fig. 10. Lacosamide amounts at the production date and during the storage period of 6 months (Mean ± SE; n = 3).** EL1, EL2, and EL3, Eudragit S 100 based formulations; CL1, CL2, and CL3, carboxymethyl cellulose-based formulations.
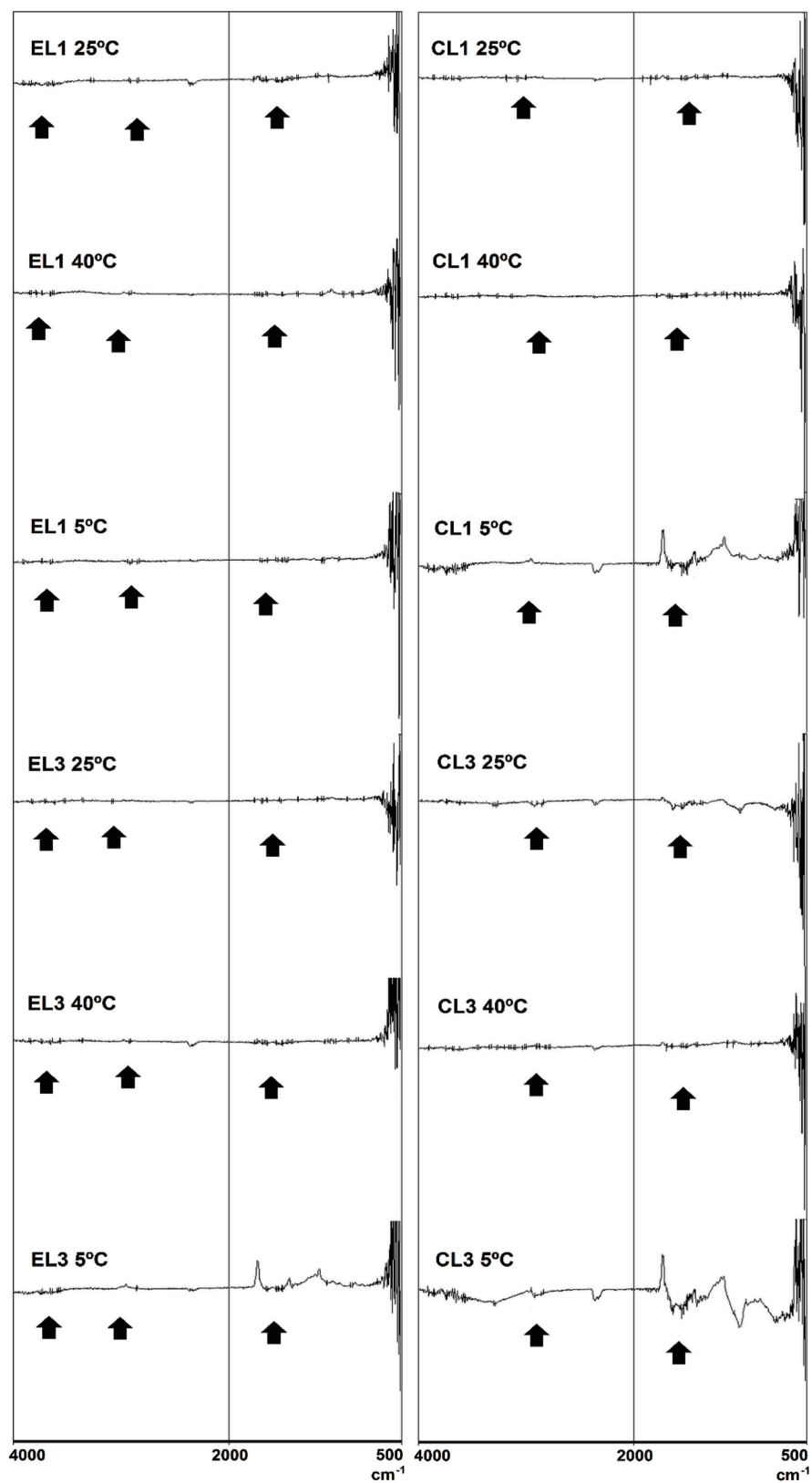
**Fig. 11. FTIR spectra of the microneedles at 6 months.** EL1, EL2, and EL3, Eudragit S 100 based formulations; CL1, CL2, and CL3, carboxymethyl cellulose-based formulations.

**Fig. 12. ¹H-NMR spectra of the microneedles at 6 months.** EL1, EL2, and EL3, Eudragit S 100 based formulations; CL1, CL2, and CL3, carboxymethyl cellulose-based formulations.
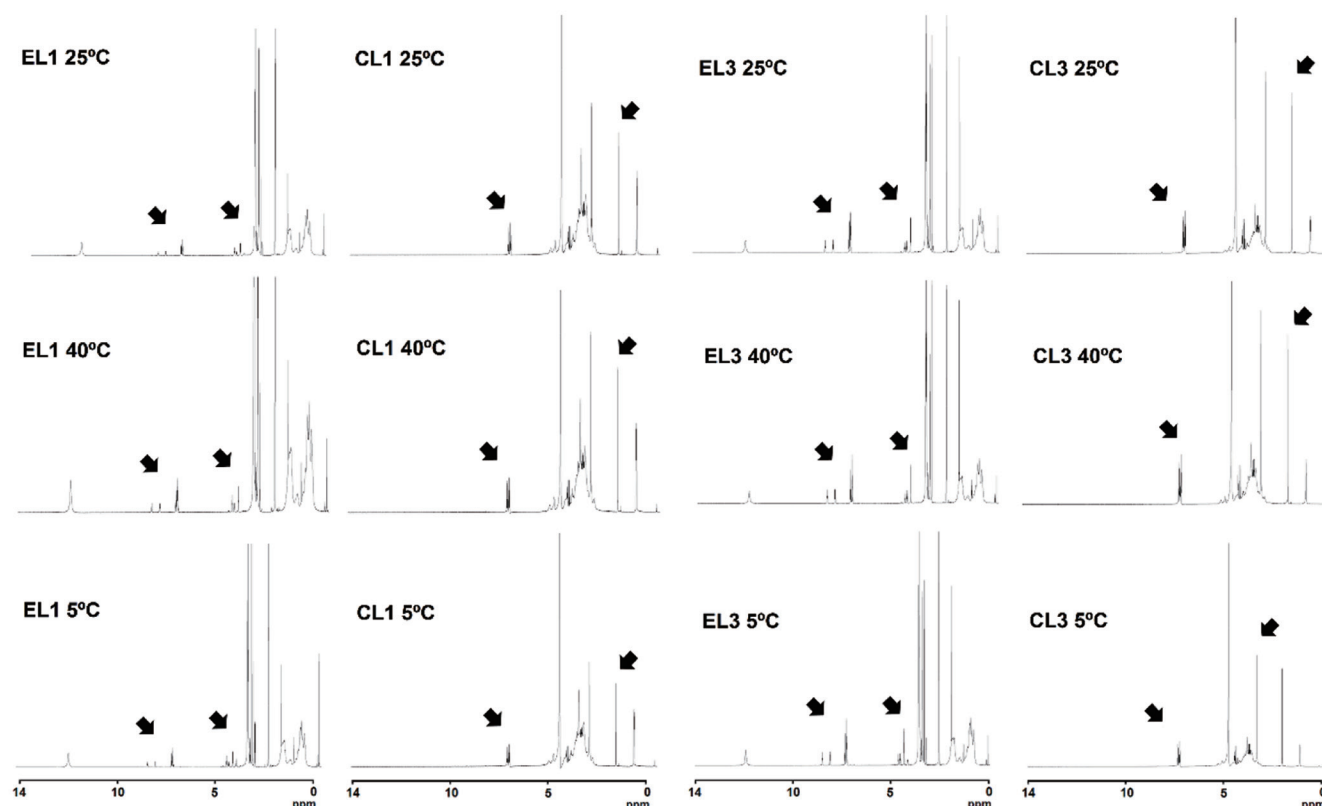
*of Exploratory Research in Pharmacology* since November 2021. The authors have no other conflicts of interest related to this publication.

**Author contributions**

Contributed to study concept and design (EB), the performance of experiments (KA), analysis and interpretation and acquisition of the data (EB and KA), assay performance and data analysis (EB and KA), drafting of the manuscript (EB, KA), critical revision of the manuscript (EB), supervision (EB).

**Data sharing statement**

No additional data are available.

**References**

[1]   Doboszewska U, Młyniec K, Wlaź A, Poleszak E, Nowak G, Wlaź P. Zinc signaling and epilepsy. Pharmacol Ther 2019;193:156–177. doi:10.1016/j.pharmthera.2018.08.013, PMID:30149099.

[2]   Stafstrom CE, Carmant L. Seizures and epilepsy: an overview for neuroscientists. Cold Spring Harb Perspect Med 2015;5(6):a022426. doi:10.1101/cshperspect.a022426, PMID:26033084.

[3]   Kamitaki BK, Minacapelli CD, Zhang P, Wachuku C, Gupta K, Catalano C, *et al*. Drug-induced liver injury associated with antiseizure medications from the FDA Adverse Event Reporting System (FAERS). Epilepsy Behav 2021;117:107832. doi:10.1016/j.yebeh.2021.107832, PMID:33626490.

[4]   Karasin B, Karasin M. Epilepsy: Clinical review and surgical options. AORN J 2017;106(5):393–414. doi:10.1016/j.aorn.2017.09.003, PMID:29107258.

[5]   Berg AT, Berkovic SF, Brodie MJ, Buchhalter J, Cross JH, van Emde Boas W, *et al*. Revised terminology and concepts for organization of seizures and epilepsies: Report of the ILAE Commission on Classification and Terminology, 2005-2009. Epilepsia 2010;51(4):676–685. doi:10.1111/j.1528-1167.2010.02522.x, PMID:20196795.

[6]   Rogawski MA, Tofighy A, White HS, Matagne A, Wolff C. Current understanding of the mechanism of action of the antiepileptic drug lacosamide. Epilepsy Res 2015;110:189–205. doi:10.1016/j.eplepsyres.2014.11.021, PMID:25616473.

[7]   Villanueva V, Giráldez BG, Toledo M, De Haan GJ, Cumbo E, Gambardella A, *et al*. Lacosamide monotherapy in clinical practice: A retrospective chart review. Acta Neurol Scand 2018;138(3):186–194. doi:10.1111/ane.12920, PMID:29542107.

[8]   Cawello W, Stockis A, Andreas JO, Dimova S. Advances in epilepsy treatment: lacosamide pharmacokinetic profile. Ann N Y Acad Sci 2014;1329:18–32. doi:10.1111/nyas.12513, PMID:25167889.

[9]   Halford JJ, Lapointe M. Clinical perspectives on lacosamide. Epilepsy Curr 2009;9(1):1–9. doi:10.1111/j.1535-7511.2008.01273.x, PMID:19396339.

[10]  Gáll Z, Vancea S. Distribution of lacosamide in the rat brain assessed by *in vitro* slice technique. Arch Pharm Res 2018;41(1):79–86. doi:10.1007/s12272-017-0966-2, PMID:29019022.

[11]  Koo TS, Kim SJ, Ha DJ, Baek M, Moon H. Pharmacokinetics, brain distribution, and plasma protein binding of the antiepileptic drug lacosamide in rats. Arch Pharm Res 2011;34(12):2059–2064. doi:10.1007/s12272-011-1208-7, PMID:22210031.

[12]  Jadhav K, Gambhire M, Shaikh I, Kadam V, Pisal S. Nasal drug deliv-

ery system-factors affecting and applications. Curr Drug Ther 2007; 2(1):27–38. doi:10.2174/157488507779422374.

[13] Appasaheb PS, Manohar SD, Bhanudas SR. A Review on ıntranasal drug delivery system. J Adv Pharm Educ Res 2013;3(4):333–346.

[14] Misra A, Kher G. Drug delivery systems from nose to brain. Curr Pharm Biotechnol 2012;13(12):2355–2379. doi:10.2174/138920112803341752, PMID:23016642.

[15] Kaur P, Garg T, Rath G, Goyal AK. *In situ* nasal gel drug delivery: A novel approach for brain targeting through the mucosal membrane. Artif Cells Nanomed Biotechnol 2016;44(4):1167–1176. doi:10.3109/21691401. 2015.1012260, PMID:25749276.

[16] Ravi G, Gupta NV, Gowrav MP. A comprehensive review on microneedles - an archetype swing in transdermal drug delıvery. Indo Am J Pharm Res 2017;7:7399–7416.

[17] Ita K. Dissolving microneedles for transdermal drug delivery: Advances and challenges. Biomed Pharmacother 2017;93:1116–1127. doi:10.1016/j.biopha.2017.07.019, PMID:28738520.

[18] Rzhevskiy AS, Singh TRR, Donnelly RF, Anissimov YG. Microneedles as the technique of drug delivery enhancement in diverse organs and tissues. J Control Release 2018;270:184–202. doi:10.1016/j.jconrel.2017.11.048, PMID:29203415.

[19] Ita K. Ceramic microneedles and hollow microneedles for transdermal drug delivery: Two decades of research. J Drug Deliv Sci Technol 2018;44:314–322. doi:10.1016/j.jddst.2018.01.004.

[20] Tuan-Mahmood TM, McCrudden MT, Torrisi BM, McAlister E, Garland MJ, Singh TR, *et al*. Microneedles for intradermal and transdermal drug delivery. Eur J Pharm Sci 2013;50(5):623–637. doi:10.1016/j.ejps. 2013.05.005, PMID:23680534.

[21] Larrañeta E, Lutton REM, Woolfson AD, Donnelly RF. Microneedle arrays as transdermal and intradermal drug delivery systems: Materials science, manufacture and commercial development. Mater Sci Eng R 2016;104:1–32. doi:10.1016/j.mser.2016.03.001.

[22] Lee C, Kim H, Kim S, Lahiji SF, Ha NY, Yang H, *et al*. Comparative study of two droplet-based dissolving microneedle fabrication methods for skin vaccination. Adv Healthc Mater 2018;7(11):e1701381. doi:10.1002/adhm.201701381, PMID:29663698.

[23] Wang M, Hu L, Xu C. Recent advances in the design of polymeric microneedles for transdermal drug delivery and biosensing. Lab Chip 2017;17(8):1373–1387. doi:10.1039/c7lc00016b, PMID:28352876.

[24] Sharma S, Hatware K, Bhadane P, Sindhikar S, Mishra DK. Recent advances in microneedle composites for biomedical applications: Advanced drug delivery technologies. Mater Sci Eng C Mater Biol Appl 2019;103:109717. doi:10.1016/j.msec.2019.05.002, PMID:31349403.

[25] Duarah S, Sharma M, Wen J. Recent advances in microneedle-based drug delivery: Special emphasis on its use in paediatric population. Eur J Pharm Biopharm 2019;136:48–69. doi:10.1016/j.ejpb.2019.01.005, PMID:30633972.

[26] Waghule T, Singhvi G, Dubey SK, Pandey MM, Gupta G, Singh M, *et al*. Microneedles: A smart approach and increasing potential for transdermal drug delivery system. Biomed Pharmacother 2019;109:1249–1258. doi:10.1016/j.biopha.2018.10.078, PMID:30551375.

[27] Mogusala NR, Devadasu VR, Venisetty RK. Fabrication of microneedle molds and polymer based biodegradable microneedle patches: a novel method. Am J Drug Deliv Ther 2015;2:60–71.

[28] Larrañeta E, Moore J, Vicente-Pérez EM, González-Vázquez P, Lutton R, Woolfson AD, *et al*. A proposed model membrane and test method for microneedle insertion studies. Int J Pharm 2014;472(1-2):65–73. doi:10.1016/j.ijpharm.2014.05.042, PMID:24877757.

[29] Migdadi EM, Courtenay AJ, Tekko IA, McCrudden MTC, Kearney MC, McAlister E, *et al*. Hydrogel-forming microneedles enhance transdermal delivery of metformin hydrochloride. J Control Release 2018;285:142–151. doi:10.1016/j.jconrel.2018.07.009, PMID:29990526.

[30] Sreenivasulu V, Rao DR, Uma Maheswari BN, Das SK, Krishnaiah A. Development and validation of a stability-indicating RP - HPLC method for determination of lacosamide. Res J Pharm Biol Chem Sci 2011;57(2):1–11. doi:10.21608/bfpc.2019.9952.1016.

[31] European Medicines Agency. ICH Q2 (R1) Validation of analytical procedures: text and methodology. Amsterdam: European Medicines Agency;1995. Available from: www.ema.europa.eu/en/ich-q2-r1-validation-analytical-procedures-text-methodology#current-effective-version-section. Accessed January 18, 2022.

[32] Başaran E. Ocular application of dirithromycin ıncorporated polymeric nanoparticles: an *in vitro* evaluation. Turk J Pharm Sci 2017;14(2):191–200. doi:10.4274/tjps.69855, PMID:32454613.

[33] Abdelnabi DM, Abdallah MH, Elghamry HA. Buspirone hydrochloride loaded ın situ nanovesicular gel as an anxiolytic nasal drug delivery system: *in vitro* and animal studies. AAPS PharmSciTech 2019;20(3):134–148. doi:10.1208/s12249-018-1211-0, PMID:30830481.

[34] Andersen TE, Andersen AJ, Petersen RS, Nielsen LH, Keller SS. Drug loaded biodegradable polymer microneedles fabricated by hot embossing. Microelectron Eng 2018;195:57–61. doi:10.1016/j.mee.2018. 03.024.

[35] Zuo J, Gao Y, Bou-Chacra N, Löbenberg R. Evaluation of the DD-Solver software applications. Biomed Res Int 2014;2014:204925. doi:10.1155/2014/204925, PMID:24877067.

[36] Li J, Zhou Y, Yang J, Ye R, Gao J, Ren L, *et al*. Fabrication of gradient porous microneedle array by modified hot embossing for transdermal drug delivery. Mater Sci Eng C Mater Biol Appl 2019;96:576–582. doi:10.1016/j.msec.2018.11.074, PMID:30606567.

[37] Han CS, Kim S, Oh DW, Yoon JY, Park ES, Rhee YS, *et al*. Preparation, characterization, and stability evaluation of taste-masking lacosamide microparticles. Materials (Basel) 2019;12(6):1000. doi:10.3390/ma12061000, PMID:30917621.

[38] Mehta R, Chawla A, Sharma P, Pawar P. Formulation and *in vitro* evaluation of Eudragit S-100 coated naproxen matrix tablets for colon-targeted drug delivery system. J Adv Pharm Technol Res 2013;4(1):31–41. doi:10.4103/2231-4040.107498, PMID:23662280.

[39] Vlachou M, Kikionis S, Siamidi A, Kyriakou S, Tsotinis A, Ioannou E, *et al*. Development and characterization of eudragit®-based electrospun nanofibrous mats and their formulation into nanofiber tablets for the modified release of furosemide. Pharmaceutics 2019;11(480):1–13. doi:10.3390/pharmaceutics11090480, PMID:31533252.

[40] Malik NS, Ahmad M, Minhas MU. Cross-linked β-cyclodextrin and carboxymethyl cellulose hydrogels for controlled drug delivery of acyclovir. PLoS One 2017;12(2):e0172727. doi:10.1371/journal.pone. 0172727, PMID:28245257.

[41] Tufan M, Uraz E, Tosun Ç, Gerçel HF. Synthesis and characterization of carboxymethyl cellulose fılm from pistachıo shells. Int J Adv Sci Eng Technol 2016;4(1):153–155.

[42] Park SJ, Kim KS. Investigation of drug delivery behaviors by NMR spectroscopy. Struct Relatsh Stud Drug Dev by NMR Spectrosc 2011;1:36–66. doi:10.2174/978160805164911101010036.

[43] Yin J, Xiang C, Song X. Nanoencapsulation of psoralidin via chitosan and Eudragit S100 for enhancement of oral bioavailability. Int J Pharm 2016;510(1):203–209. doi:10.1016/j.ijpharm.2016.05.007, PMID:271 54253.

[44] Choi IJ, Kang A, Ahn MH, Jun H, Baek SK, Park JH, *et al*. Insertion-responsive microneedles for rapid intradermal delivery of canine influenza vaccine. J Control Release 2018;286:460–466. doi:10.1016/j.jconrel.2018.08.017, PMID:30102940.

[45] European Medicines Agency. ICH Q1A-R2, I. Stability testing of new drug substances and products. Definitions London: European Medicines Agency;2003. doi:10.32388/yokp53. Available from: https:// available from: https://www.ema.europa.eu/en/documents/scientific-guideline/ich-q-1-r2-stability-testing-new-drug-substances-products-step-5_en.pdf. Accessed January 18, 2022.

[46] Kathe K, Kathpalia H. Film forming systems for topical and transdermal drug delivery. Asian J Pharm Sci 2017;12(6):487–497. doi:10.1016/j.ajps.2017.07.004, PMID:32104362.

[47] Kamel S, Ali N, Jahangir K, Shah SM, El-Gendy AA. Pharmaceutical significance of cellulose: A review. Express Polym Lett 2008;2:758–778. doi:10.3144/expresspolymlett.2008.90.

[48] Khan MZ, Stedul HP, Kurjaković N. A pH-dependent colon-targeted oral drug delivery system using methacrylic acid copolymers. II. Manipulation of drug release using Eudragit L100 and Eudragit S100 combinations. Drug Dev Ind Pharm 2000;26(5):549–554. doi:10.1081/ddc-100101266, PMID:10789067.

[49] Chen W, Wang C, Yan L, Huang L, Zhu X, Chen B, *et al*. Improved polyvinylpyrrolidone microneedle arrays with non-stoichiometric cyclodextrin. J Mater Chem B 2014;2(12):1699–1705. doi:10.1039/c3tb21698e, PMID:32261399.

[50] Seon-Woo HS, Kim HJ, Roh JY, Park JH. Dissolving microneedle sys-

tems for the oral mucosal delivery of triamcinolone acetonide to treat aphthous stomatitis. Macromol Res 2019;27:282–289. doi:10.1007/s13233-019-7031-6.

[51] Rojek B, Wesolowski M. DSC supported by factor analysis as a reliable tool for compatibility study in pharmaceutical mixtures. J Therm Anal Calorim 2019;138:4531–4539. doi:10.1007/s10973-019-08223-7.

[52] El-Sayed S, Mahmoud KH, Fatah AA, Hassen A. DSC, TGA and dielectric properties of carboxymethyl cellulose/polyvinyl alcohol blends. Phys B Condens Matter 2011;406(21):4068–4076. doi:10.1016/j.physb.2011.07.050.

[53] Mali KK, Dhawale SC, Dias RJ, Dhane NS, Ghorpade VS. Citric acid crosslinked carboxymethyl cellulose-based composite hydrogel films for drug delivery. Indian J Pharm Sci 2018;80:657–667. doi:10.4172/pharmaceutical-sciences.1000405.

[54] Gamal AB, Hassan AA. & Nahas HMEl. Optimization and Characterization of Eudragit S 100 Microsponges of Fluconazole. Int J Trend Res Dev 2016;3:141–149.

[55] Rohman A. Application of fourier transform ınfrared spectroscopy for quality control of pharmaceutical products: a review. Indones J Pharm 2013;23(1):1–8. doi:10.14499/indonesianjpharm23iss1pp1-8.

[56] Park JH, Allen MG, Prausnitz MR. Polymer microneedles for controlled-release drug delivery. Pharm Res 2006;23(5):1008–1019. doi:10.1007/s11095-006-0028-9, PMID:16715391.

[57] Peppas NA, Narasimhan B. Mathematical models in drug delivery: how modeling has shaped the way we design new drug delivery systems. J Control Release 2014;190:75–81. doi:10.1016/j.jconrel.2014.06.041, PMID:24998939.

[58] Shaikh HK, Kshirsagar R, Patil SG. Mathematical models for drug release characterization: a review. World J Pharm Pharm Sci 2015;4(4):324–338.

[59] Bruschi ML, editor. Mathematical models of drug release. Strategies to Modify the Drug Release from Pharmaceutical Systems. Woodhead Publishing. 2015:63–86. doi:10.1016/B978-0-08-100092-2.00005-9.

[60] Mourdikoudis S, Pallares RM, Thanh NTK. Characterization techniques for nanoparticles: comparison and complementarity upon studying nanoparticle properties. Nanoscale 2018;10(27):12871–12934. doi:10.1039/c8nr02278j, PMID:29926865.

[61] Abdussalam S, Mohamed S, Pedro L, Gae C, Malika LS, Hassan O. Study of interaction between tiagabine HCl and 2-HPβCD: Investigation of inclusion process. J Incl Phenom Macrocycl Chem 2010;68(1-2):55–63. doi:10.1007/s10847-009-9732-5.

[62] Abilova GK, Kaldybekov DB, Ozhmukhametova EK, Saimova AZ, Kazybayeva DS, Irmukhametova GS, *et al*. Chitosan/poly(2-ethyl-2-oxazoline) films for ocular drug delivery: Formulation, miscibility, *in vitro* and *in vivo* studies. Eur Polym J 2019;116:311–320. doi:10.1016/j.eurpolymj.2019.04.016.